On Small-Signal Stability of Wind Power System with Full-Load Converter Interfaced Wind Turbines

Knüppel, Thyge; Akhmatov, Vladislav; Nielsen, Jørgen Nygård; Jensen, Kim H.; Dixon, Andrew; Østergaard, Jacob

Published in:
Proceedings of WINDPOWER 2010 Conference & Exhibition

Publication date:
2010

Document Version
Publisher's PDF, also known as Version of record

On Small-Signal Stability of Wind Power System with Full-Load Converter Interfaced Wind Turbines

Thyge Knüppel, Vladislav Akhmatov, Jørgen N. Nielsen, Kim H. Jensen, Andrew Dixon, Jacob Østergaard

***Abstract*—Small-signal stability analysis of power system oscillations is a well established field within power system analysis, but not much attention has yet been paid to systems with a high penetration of wind turbines and with large wind power plants. In this paper an analysis is presented which assess the impact of full-load converter interfaced wind turbines on power system small-signal stability. The study is based on a 7 generator network with lightly damped inter-area modes. A detailed wind turbine model with all grid relevant control functions is used in the study. Furthermore is the wind power plant (WPP) equipped with a WPP voltage controller and comparisons are presented. The models of wind turbine and WPP voltage controller are kindly provided by Siemens Wind Power A/S for this work. The study is based on modal analysis which are complemented with simulations on the nonlinear system.**

***Index Terms*—wind turbines, wind power plant, wind power plant controller, power systems, small-signal stability, modal analysis**

I. Introduction

With the rapid development in installed capacity of wind power and with the increasing size of each installation, the role and impact of wind power on power system operation is changing. In 2008 in USA alone 8.5 GW of new wind power based generation capacity was installed which accounts for over 40 % of the total capacity added in USA in 2008 [1]. In grid codes from some transmission system operators this development is already noted, given that large wind power plants (WPP) are termed power park modules and must comply with similar requirements to those for other generation units. In continuation of this, large WPPs are often equipped with a supervisory voltage and frequency controller, i.e. a controller on park level designed to coordinate the response of the individual units in the park. The effect and intention of such supervisory controllers on park level is that the combined responses of the wind turbines (WT), evaluated at the interface between the WPP and the power system, are comparable to other power plants. The ability of WPPs to deliver active power reserves are treated in a number of publications [2]–[5], as well as voltage and reactive power control [6], [7]. In some countries, for instance Denmark, WPPs are already applied for ancillary services, e.g. frequency reserve.

Regarding power system stability investigations, considerable attention has been paid to low voltage fault-ride-through (FRT) capabilities of the WTs, i.e. the ability of the WTs to stay connected during external disturbances in the grid and provide necessary voltage support [7]–[9]. With increasing penetration of wind power and increasing size of each installed WPP new stability considerations arise. A topic of increasing importance is the effect of WPPs on power system small-signal stability, including influence on power system oscillations.

The damping of critical inter-area oscillations is affected by a number of factors such as network topography, generator excitation control, HVDC control, transmission line power flows, etc. [10]. Also, the presence of non-synchronous generation units reportedly can have an impact on the damping of inter-area oscillations. In [11]–[13] comparisons are presented of the influence on power system oscillations of WPPs based on fixed-speed induction generators (FSIG) and doubly fed induction generators (DFIG). In the studies it is generally found that FSIG WTs increase the damping of the power oscillations. References [11], [13] also report increased damping from the DFIG machine while [12] notes that the DFIG does not have any significant effect on the damping.

In [14] the influence is analyzed of the voltage/VAR control mode of DFIG based WPPs on inter-area oscillations. The study found that increasing the penetration of wind power generally had a favorable effect, with increased frequency and damping of the inter-area mode between a weak and a stronger system. With the WPP in voltage control mode [14] found that, for some parameter-set, an adverse interaction is noticed; it is, however, noted that these effects can be avoided with appropriate tuning of the voltage controller.

In [15], [16] a generic small-signal stability model is developed for fixed- and variable-speed WTs with corresponding collector and utility grid where the units are connected. The approach is based on sensitivity analysis and singular value decomposition.

A few publications have investigated the possibility of using variable-speed WPPs actively to damp power system oscillations [17]–[20]. In a recent PhD thesis by Elkington it is concluded that DFIG based WPPs can provide a positive contribution to damping of power system oscillations by adding an auxiliary controller [21].

In this paper the impact of full-load converter interfaced wind turbines on small-signal stability, e.g. participation in power system oscillations, is investigated. The system is analyzed for the WPP with and without WPP voltage con-

T. Knüppel is with Siemens Wind Power A/S, DK-7330 Brande, Denmark and Centre for Electric Technology, Technical University of Denmark, DK-2800 Lyngby, Denmark (thyge.knuppel@siemens.com)

V. Akhmatov, J. N. Nielsen, and K. H. Jensen are with Siemens Wind Power A/S, DK-7330 Brande, Denmark

A. Dixon is with National Grid Electricity Transmission plc (National Grid), Warwick CV34 6DA, UK

J. Østergaard is with Centre for Electric Technology, Technical University of Denmark, DK-2800 Lyngby, Denmark

troller. The analysis is based on a 7 generator network, which illustrates some aspects of the dynamic behavior of the UK power system, namely inter-area oscillations between major areas of the system.

The paper is organized as follows. In section II the basis for the analysis is established with a description of modal analysis and power system oscillations. Section III presents the study case, the analyzed WT concept, and the base characteristics of the study case, while section IV presents the case studies performed and the results of the analysis. Finally, the discussion and conclusion are found in sections V and VI, respectively.

II. Method

Power system oscillations are inherent in interconnected power systems based on synchronous generators [22]. Power system oscillations and the application of eigenvalue analysis as means of analysis are well described in the literature, e.g. [10], [23]. Another approach is to base the analysis on signal processing of measured data [24]–[26]. When analyzing very large systems this measurement based approach has the advantage that it is not dependent on the accuracy of a large dynamic model.

A. Eigenvalue Analysis

The analysis is based on the nonlinear set of system equations, dynamic relations as well as network equations, which are linearized in an operating point to obtain a linear system in the classical state space form

$$\begin{aligned} \dot{\mathbf{x}} &= \mathbf{A}\mathbf{x} + \mathbf{B}\mathbf{u} \\ \mathbf{y} &= \mathbf{C}\mathbf{x} + \mathbf{D}\mathbf{u} \end{aligned} \tag{1}$$

where $\mathbf{x}^{n\times 1}$ is the state vector, $\mathbf{u}^{r\times 1}$ the input vector, $\mathbf{y}^{m\times 1}$ the output vector, $\mathbf{A}^{n\times n}$ is the system state matrix, $\mathbf{B}^{n\times r}$ the input matrix, $\mathbf{C}^{m\times n}$ the output matrix, and $\mathbf{D}^{m\times r}$ the feed forward matrix. To analyze the dynamic performance of the system in (1) it is often useful to perform a similarity transformation to diagonalize $\mathbf{A}$, i.e. decouple the system dynamics.

$$\mathbf{A}\boldsymbol{\phi}_i = \lambda_i \boldsymbol{\phi}_i, \quad \text{for } i = 1, 2, \ldots, n \tag{2}$$

where the eigenvalue, λ_i, is found as the solution of

$$\det(\mathbf{A} - \lambda_i \mathbf{I}) = 0 \tag{3}$$

and where $\mathbf{I}^{n\times n}$ is the identity matrix and $\boldsymbol{\phi}_i^{n\times 1}$ the right eigenvector for the ith eigenvalue, also commonly referred to as the mode-shape for the ith mode. Similar to the formulation in (2), the left eigenvector is defined as

$$\boldsymbol{\psi}_i \mathbf{A} = \lambda_i \boldsymbol{\psi}_i, \quad \text{for } i = 1, 2, \ldots, n \tag{4}$$

where $\boldsymbol{\psi}_i^{1\times n}$ is the left eigenvector for the ith eigenvalue.

In compact notation for all n eigenvalues, the right and left eigenvector matrices are defined as

$$\boldsymbol{\Phi} = [\boldsymbol{\phi}_1\ \boldsymbol{\phi}_2\ \ldots\ \boldsymbol{\phi}_n] \quad \boldsymbol{\Psi} = \left[\boldsymbol{\psi}_1^T\ \boldsymbol{\psi}_2^T\ \ldots\ \boldsymbol{\psi}_n^T\right]^T \tag{5}$$

Further, for power system studies the eigenvector matrices are usually scaled to satisfy $\boldsymbol{\Psi}\boldsymbol{\Phi} = \mathbf{I}$.

The right eigenvector, $\boldsymbol{\phi}_i$, describes how the activity of the ith mode is distributed on the n state variables, while the left eigenvector, $\boldsymbol{\psi}_i$, weighs the contribution of the n state variables on the ith mode. The entrywise product of $\boldsymbol{\phi}_i$ and $\boldsymbol{\psi}_i^T$ is thus a measure of the importance of the states within the individual modes and is referred to as the participation factors

$$\mathbf{p}_i = [\boldsymbol{\phi}_{1i}\boldsymbol{\psi}_{i1}\ \boldsymbol{\phi}_{2i}\boldsymbol{\psi}_{i2}\ \ldots\ \boldsymbol{\phi}_{ni}\boldsymbol{\psi}_{in}]^T, \tag{6}$$

or in compact notation

$$\mathbf{P} = \boldsymbol{\Phi} \otimes \boldsymbol{\Psi}^T \tag{7}$$

where $\otimes$ denotes the entrywise product of two equal sized matrices, and $\mathbf{P}^{n\times n}$ is the participation factor matrix.

The eigenvalues provide important information on the dynamics of the system, i.e. the frequency and damping of any oscillations. If the ith eigenvalue is given as $\lambda_i = a \pm jb$, the natural frequency, ω_n, the damped frequency, ω_d, and the damping ratio, ζ, are defined as

$$\omega_n = \sqrt{a^2 + b^2} \quad \left[\frac{\text{rad}}{\text{sec}}\right], \quad \omega_d = b \quad \left[\frac{\text{rad}}{\text{sec}}\right], \quad \zeta = \frac{-a}{\omega_n} \quad [-]$$

From classical control theory of continuous time systems, it is given that mode λ_i is asymptotically stable only if $a < 0$.

It should be remembered that power systems in general are nonlinear while the modal analysis is based on a linear approach. Thus, the results from the modal analysis are only valid in proximity of the linearization point and should be perceived as a snapshot of the dynamic system behavior. The method of normal forms offer a framework for extending the modal analysis to include higher order terms and thereby capture dynamics not captured by a linear model [27], [28]. This method is especially important for stressed, highly nonlinear power systems which are not accurately described by the linear approximation in (1). Other means of ensuring the validity of the linear analysis is to complement with nonlinear time-domain simulations after which the dynamic response is evaluated.

To gain deeper insight into the dynamic behavior of the system, a series of modal analysis is often conducted where certain system parameter(s) are gradually changed. Analyzing the movement of the eigenvalues in the complex plane reveals the influence of the varied parameter to overall system dynamics and small-signal stability.

B. Power System Oscillations

In an interconnected power system the speed of the synchronous generators will constantly adjust according to the imbalance between generation and demand, where a production surplus will cause overspeeding of the generators; and vice-versa. It must be noted that the applied governor control is to keep the synchronous speed, i.e. the nominal grid frequency within a required narrow range of operation.

Power system oscillations are typically divided into three groups depending on its global (or local) scale.

- inter-area oscillations where a group of generators in one area oscillates against a group of machines in another area, typically $f \in [0.1\ 0.3]$ Hz

- intra-area oscillations where a group of generators in one area oscillates against a group of machines in the same area, typically $f \in [0.4\ 0.7]$ Hz
- local-area or intermachine oscillations involve generators which are located close to each other, typically $f \in [0.7\ 2.0]$ Hz. This includes adverse interaction between equipment control systems.

Many factors, beside the frequency of oscillation, do, however, determine the nature of the oscillations, and the concepts of mode-shape and participation factor are used to correctly identify the source, nature, and significance of a mode.

III. Study Case

A. Case Network

The study is based on the 18 node, 7 generator system depicted in Fig. 1, which furthermore consists of 6 loads, and an aggregated WPP with corresponding collector grid. The system represents a large network that has been reduced to a small number of nodes. In TABLE VIII the generator ratings, transformer reactances, and load distributions are given, while the synchronous machine dynamic data and the network parameters are given in TABLE IX and XI, respectively.

The network model has been developed in collaboration with National Grid as an extension of the three generator system presented in [11] to achieve a higher level of flexibility and numerical stability. The network model is tuned for a light load situation and the distribution of load and generation implies a southbound power flow of approximately 1 900 MW. Note that the model does not accurately represent particular aspects of the UK network, and hence should not be used to draw conclusions regarding the performance of this network. The developed model does, however, assist in the understanding of power oscillations between major areas of the UK power system.

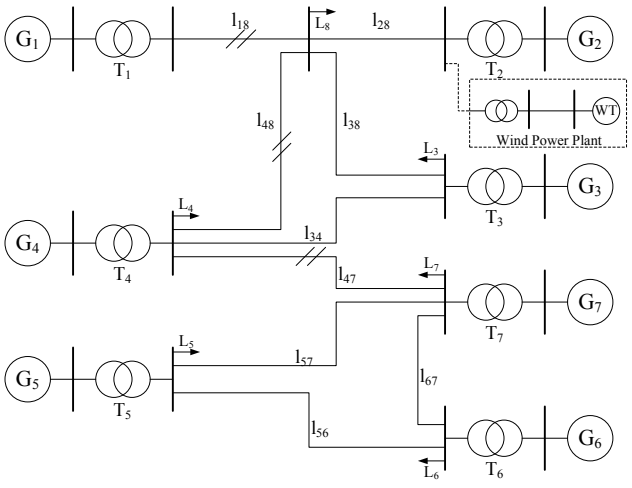

Fig. 1. Single-line diagram of the analyzed case network.

B. Wind Turbine Technology

The WT concept for this study is a variable-speed, pitch controlled, full-load converter interfaced WT and is illustrated in Fig. 2 and further described in [29]. A block diagram showing the overall connections is shown in Fig. 3. The applied model is kindly provided by Siemens Wind Power A/S being a key market player of such variable-speed WTs.

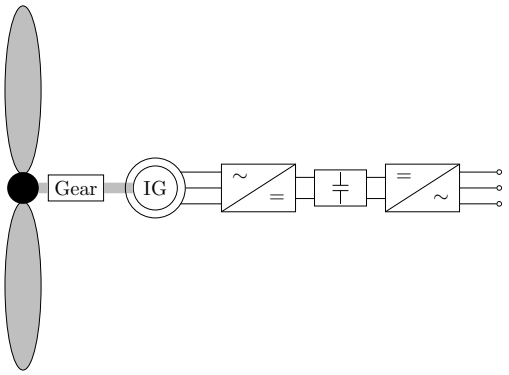

Fig. 2. Wind turbine concept used in the analysis, i.e. full-load converter interfaced WT.

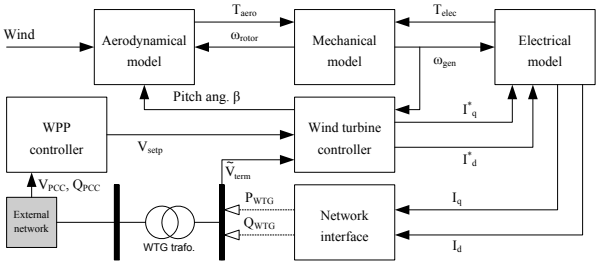

Fig. 3. Overall block diagram of the WT model.

The applied model includes:

- *Aerodynamic model*. A variable wind speed aerodynamic model which includes power coefficient with pitch angle and tip-speed ratio.
- *Shaft model*. Implements a two-mass model of rotor, gearbox, and generator.
- *Converter system*. The WT converter system comprises a generator side and a network side converter including all required control of the injected active and reactive power as well as DC link voltage control.
- *DC link*. Implements the link, including the DC capacitance, between the machine and the network side converter.
- *Fault ride through*. Monitors for system faults and shapes the current injection into the grid upon detection.

In the study, an aggregated WT model is used and the analysis thus only considers the main interaction between the power system and the WPP.

C. Wind Power Plant Collector Grid

The collector grid is modeled as a T-equivalent with the entire capacitance lumped as a shunt and with half the inductance and half the resistance as a series impedance on each side. For $P_{\mathrm{WPP}} = 180$ MW the network parameters are

given in TABLE X. The collector grid parameters are scaled according to the size of the WPP such that the same voltage profile is achieved, i.e.

$$z_{\text{scale}} = \frac{S^B_{\text{base}}}{S_{\text{base,WPP}}} \qquad R = z_{\text{scale}} R^B$$

$$X_L = z_{\text{scale}} X^B_L \qquad B_C = \frac{B^B_C}{z_{\text{scale}}}$$

where the superscript $.^B$ refers to the values in TABLE X with $P_{\text{WPP}} = 180$ MW.

D. Wind Power Plant Voltage Controller

The WPP voltage controller is an outer, corrective controller that controls the voltage at the point of common connection (PCC) at the interface to the power system. The WPP voltage controller distributes voltage set-points to the individual WTs based on the conditions at the PCC, where the WT voltage controller controls the voltage at the WT terminals according to its set-point.

The block diagram of the WPP voltage controller is shown in Fig. 4 and the relation to the WT system is shown in the block diagram in Fig. 3. The droop controller prevents chasing of adjacent units both controlling the voltage by dividing the responsibility between the units. Furthermore, the droop controller ensures that a predictable amount of reactive power is delivered for a given deviation from the nominal voltage. The applied model of the WPP voltage controller has been kindly provided by Siemens Wind Power for this analysis, although Siemens Wind Power does not necessarily apply exactly the same control.

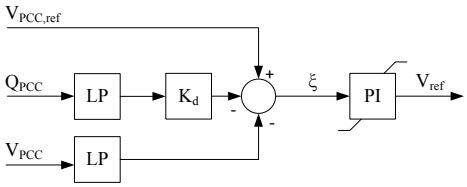

Fig. 4. Block diagram of the WPP voltage droop controller. LP: Low-Pass filter, PI: PI-controller.

The operation of the WPP voltage controller is dependent on the strength of the grid and the controller must be carefully tuned for the conditions at the PCC. For this analysis, a 4 % droop, i.e. $K_d = 0.04$, is used and the WPP voltage controller is tuned to deliver 90 % of its response within 1 second in a well-damped manner [30].

A simulation is presented in Fig. 5 where a step-change is applied to the set-point of the exciter of the nearby generator G_2. The shown step-response is with $P_{\text{WPP}} = 504$ MW. As shown in Fig. 4 the WPP responds in a fast and well-damped manner, delivering the scheduled reactive power within 1 second. The set-point change at G_2 inflicts a perturbation in the electromagnetic torque at G_2, noticed by the swing in delivered active power. For the WPP the reactive power output is increased without affecting the delivery of active power.

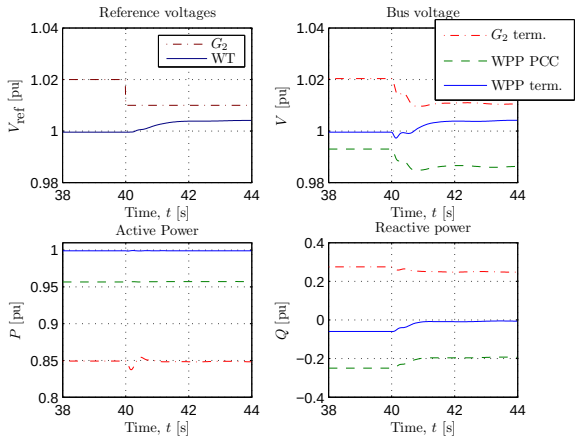

Fig. 5. Time simulation showing the response of the WPP voltage controller to a step on the voltage reference on G_2. $P_{\text{WPP}} = 504$ MW.

E. Generator Models

The synchronous generators are modeled as round rotor machines using the standard RMS model. The generators are aggregated machines, each representing several smaller and larger generation units; the total capacity for each unit is given in TABLE VIII and the parameters for the dynamic model in TABLE IX.

Parameters for the synchronous machines with corresponding exciter- and PSS models are selected to represent the dominant unit type in each area. Furthermore is each generator equipped with a standard IEEEG0 governor. Parameters, exciter- and PSS models have kindly been provided by National Grid for this study.

F. Characteristics of Case Network

A list of dominant eigenvalues is given in TABLE I. Three lightly damped inter-area modes are present in the system, λ_{1-3}; the modal characteristics are given in TABLE II and the mode shapes in Fig. 6. Furthermore are three voltage controller modes selected for closer attention, λ_{4-6}, as the analysis will show that these modes are sensitive to the size of the WPP.

TABLE I
QUALITATIVE DESCRIPTION OF DOMINANT EIGENVALUES.

λ_1	Inter-area mode between G_{1-2} and G_{3-7}
λ_2	Inter-area mode between $G_{4,7}$ and G_{5-6}
λ_3	Inter-area mode between G_4 and G_7
λ_4	Voltage controller common mode, G_1, G_2, WPP
λ_5	Voltage controller common mode, G_2, WPP
λ_6	Voltage controller common mode, G_2, WPP

TABLE II
CHARACTERISTIC FOR THREE INTER-AREA MODES IN BASE CASE WITHOUT WIND POWER.

#	λ [-]	ω_d [Hz]	ζ [-]
λ_1	$-0.275 \pm j3.10$	0.493	0.088
λ_2	$-0.658 \pm j6.26$	0.997	0.105
λ_3	$-0.643 \pm j8.83$	1.41	0.073

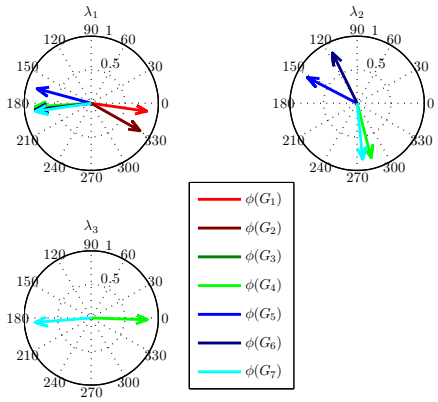

Fig. 6. Mode shape for generator speed states for three inter-area modes for the system with no wind power connected.

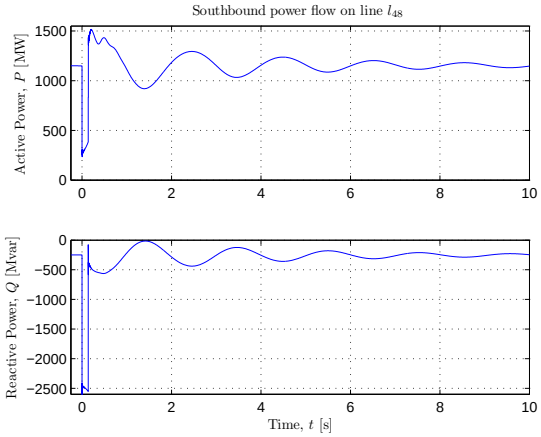

Fig. 7. Active and reactive power flow on line l_{48} after a short-circuit on one of the l_{48} lines.

In TABLE III are the participation factors for the inter-area modes shown for the generator rotor angle states. The mode shape for three inter-area modes, λ_{1-3}, are given in Fig. 6 where the characteristic 180^o displacement between oscillating groups of generators is seen. The characteristics of the inter-area modes given in TABLE I are determined from the participation factors in TABLE III and the mode shapes in Fig. 6.

TABLE III
NORMALIZED ROTOR ANGLE PARTICIPATION FACTORS FOR THE INTER-AREA MODES λ_{1-3} FOR THE SYSTEM WITH NO WIND POWER CONNECTED.

State variable	$\lvert p_{j1}\rvert$	$\lvert p_{j2}\rvert$	$\lvert p_{j3}\rvert$
$\delta\ (G_1)$	0.21	$< 10^{-2}$	$< 10^{-4}$
$\delta\ (G_2)$	0.11	$< 10^{-2}$	$< 10^{-4}$
$\delta\ (G_3)$	$< 10^{-2}$	0.01	0.01
$\delta\ (G_4)$	0.03	0.28	0.07
$\delta\ (G_5)$	0.04	0.02	$< 10^{-2}$
$\delta\ (G_6)$	0.08	0.18	$< 10^{-2}$
$\delta\ (G_7)$	0.01	0.02	0.42

The modal analysis is a linear method and it should thus be complemented with dynamic simulations on the nonlinear system. In Fig. 7 and 8 the dynamic response is shown after a three-phase short-circuit at line l_{48}. For now, there is no wind power in the system. The fault is applied midway between the busses, on a single circuit, and it is cleared after 140 ms. Fig. 7 shows the active and reactive power flow on the double circuit l_{48} during and after the short-circuit. From the dynamic response the damping ratio, ζ, and the damped frequency of oscillation, ω_d are computed as

$$\delta = \tfrac{1}{3}\ln\left(\frac{1294-1150}{1181-1150}\right) = 0.5119$$
$$\zeta = \frac{\delta}{\sqrt{\delta^2+(2\pi)^2}} = 0.081$$
$$\omega_d = \left(\tfrac{1}{3}(7.523-1.391)\right)^{-1} = 0.49$$

The short-circuit excites inter-area oscillation λ_1 between G_{1-2} and G_{3-7}, which is noted by the grouping of the generators in Fig. 8 where the generator rotor speeds are plotted, cf. mode shape plot in Fig. 6.

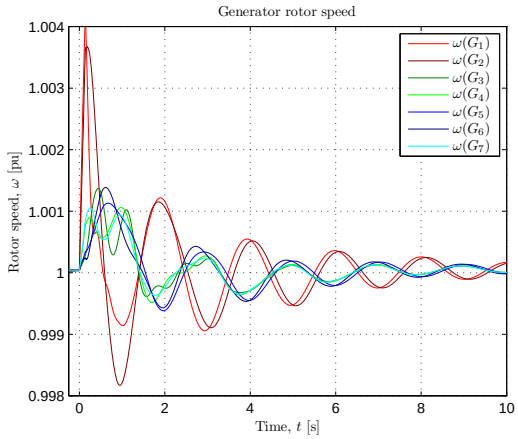

Fig. 8. Generator rotor speeds after a short-circuit on one of the l_{48} lines.

IV. SELECTED CASES

The aim of the study is to analyze the influence of increased wind power penetration on power oscillations in the system, with emphasis on the previously mentioned inter-area modes.

Two cases with a varying penetration of wind power are investigated and compared to the base case with only synchronous generation

1) P_{setp} of G_2 is reduced as penetration of wind power is increased while the MVA rating is maintained
2) MVA rating of G_2 is reduced as penetration of wind power is increased while the loading of G_2 is maintained

In all cases and for all wind power penetration levels, active power production is shifted between only G_2 and the WPP and the power flow in the system is thus unchanged.

In case 1 the introduction of wind power does not displace any conventional units and only the active power set-point is reduced to accommodate the power produced by the WPP. While in case 2, the wind power displaces conventional units

and the MVA rating of G_2 is reduced accordingly. In each case the size of the WPP is varied linearly from 36 to 1 000 MW in 10 steps.

A. Local WT Voltage Control

When only local voltage control is employed in the WPP, the WTs control to achieve a voltage of 1 pu at the terminals.

The modal characteristics of the three selected inter-area modes, λ_{1-3}, are presented in TABLE IV for $P_{\text{WPP}} = 1\,000$ MW. When compared to the modal characteristics of the base case in TABLE II it is clear that the three inter-area modes are largely unaffected by the 1 000 MW WPP.

TABLE IV
CHARACTERISTICS FOR THREE INTER-AREA MODES λ_{1-3} WITH 1 000 MW OF WIND POWER.

	#	λ [-]	ω_d [Hz]	ζ [-]
Case 1	λ_1	$-0.280 \pm j3.13$	0.498	0.089
Case 1	λ_2	$-0.663 \pm j6.26$	0.996	0.105
Case 1	λ_3	$-0.644 \pm j8.83$	1.40	0.073
Case 2	λ_1	$-0.287 \pm j3.24$	0.516	0.088
Case 2	λ_2	$-0.666 \pm j6.27$	0.997	0.106
Case 2	λ_3	$-0.644 \pm j8.83$	1.41	0.073

An overview of the complex plane with system eigenvalues, as the WPP penetration increases, is depicted in Fig. 9 for both cases. A comparison of the selected eigenvalues in TABLE I is given in Fig. 10. From Fig. 9 and Fig. 10 it should be noted that the inter-area modes, λ_{1-3}, only exhibit little movement in the complex plane, whereas the movement of the common voltage controller modes, λ_{4-6}, is more significant.

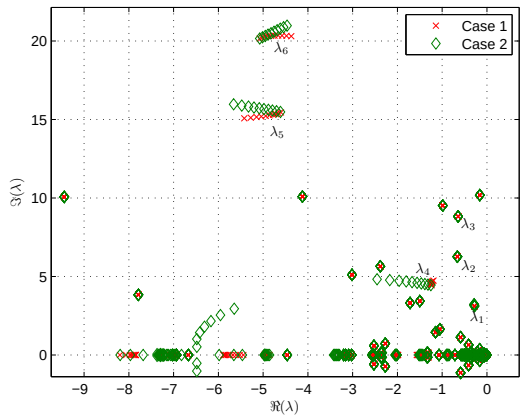

Fig. 9. System eigenvalues in the complex plane.

The participation factors measure the participation of each state variable in the eigenvalues and thus how each mode is shaped. In TABLE V selected participation factors are listed for inter-area mode, λ_1; namely, generator rotor angle states and WPP mechanical generator, rotor, and shaft states. Furthermore is the largest participation over all WPP states given. The maximum WPP participation is in both cases found in the reactive power controller. Note that only the participation factors for mode λ_1 are given, however, similar results are obtained for λ_{2-3}. It should be noticed that the participation

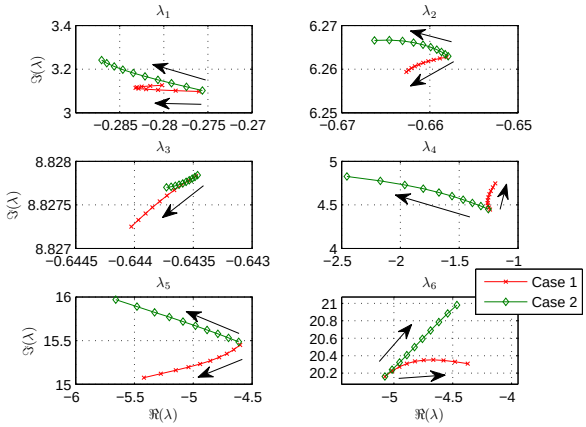

Fig. 10. Comparison of selected system eigenvalues.

factors for the WPP mechanical states are orders of magnitude smaller than those of the synchronous generators; hereby implying that the WPP does not participate in the oscillation.

TABLE V
COMPARISON OF SELECTED PARTICIPATION FACTORS FOR INTER-AREA MODE, λ_1, FOR CASE 1 AND 2. FOR THE WPP PARTICIPATION FACTORS ARE SHOWN FOR MECHANICAL GENERATOR-, ROTOR- AND SHAFT-ANGLE STATES, AND THE MAXIMUM PARTICIPATION OVER ALL WPP STATES. $P_{\text{WPP}} = 1\,000$ MW.

State variables	$\lvert p_{j1}\rvert$ case 1	$\lvert p_{j1}\rvert$ case 2
δ (G_1)	0.22	0.28
δ (G_2)	0.10	0.05
δ (G_3)	$< 10^{-2}$	$< 10^{-2}$
δ (G_4)	0.03	0.03
δ (G_5)	0.04	0.03
δ (G_6)	0.08	0.07
δ (G_7)	0.01	0.01
δ_g (WPP)	$< 10^{-7}$	$< 10^{-7}$
δ_r (WPP)	$< 10^{-5}$	$< 10^{-5}$
δ_s (WPP)	$< 10^{-5}$	$< 10^{-5}$
$\max_{\mathbf{x}}(\lvert p_1\rvert)$ (WPP)	$< 10^{-2}$	$< 10^{-2}$

For case 1 with $P_{\text{WPP}} = 1\,000$ MW, the mode shapes are given in Fig. 11 for the generator speed states for the three inter-area modes, λ_{1-3}. The inter-area characteristics in terms of generator grouping are not significantly changed by the WPP. Similar mode shapes are obtained for case 2.

B. Wind Power Plant Voltage Controller

The modal characteristics of the three selected inter-area modes, λ_{1-3}, are presented in TABLE VI for $P_{\text{WPP}} = 1\,000$ MW and with WPP voltage controller. When compared to the modal characteristics of the case with only local WT voltage control in TABLE IV, it is clear that the three inter-area modes are largely unaffected by the WPP voltage controller.

A comparison of the eigenvalue movement as the wind power penetration increases from 36 to 1 000 MW is given in Fig. 12; again only limited movement of the three inter-area modes are noticed. The mode shapes for the generator speed states for the three inter-area modes are given in Fig. 13 for

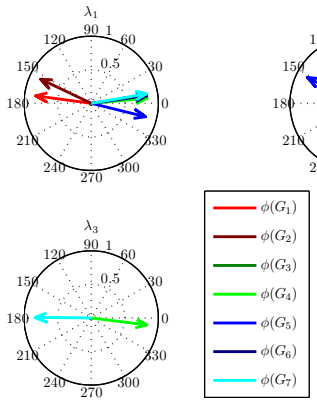

Fig. 11. Mode shape for the generator speed state for three inter-area modes. The presented mode shapes are for case 1 with $P_{\text{WPP}} = 1\,000$ MW

TABLE VI
CHARACTERISTICS FOR THREE INTER-AREA MODES λ_{1-3} WITH 1 000 MW OF WIND POWER AND WPP VOLTAGE CONTROLLER.

	#	λ [-]	ω_d [Hz]	ζ [-]
Case 1	λ_1	$-0.278 \pm j3.13$	0.499	0.088
Case 1	λ_2	$-0.663 \pm j6.26$	0.996	0.105
Case 1	λ_3	$-0.644 \pm j8.83$	1.40	0.073
Case 2	λ_1	$-0.287 \pm j3.25$	0.517	0.088
Case 2	λ_2	$-0.668 \pm j6.27$	0.997	0.106
Case 2	λ_3	$-0.644 \pm j8.83$	1.40	0.073

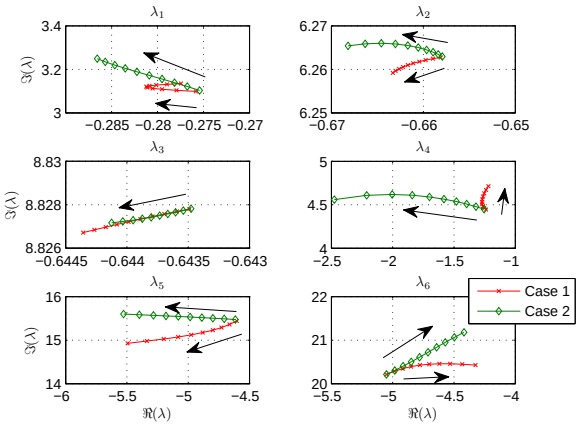

Fig. 12. Comparison of selected system eigenvalues with WPP voltage controller.

case 1 with $P_{\text{WPP}} = 1\,000$ MW. Similar results are obtained for case 2 where G_2 is gradually displaced.

In TABLE VII the participation factors are given for inter-area mode λ_1 for case 1 and 2. Similar results are found for inter-area modes λ_{2-3}. As noted in section IV-A the WPP participation in the oscillation is orders of magnitude smaller than for the synchronous machines. The largest participation factor for both case 1 and 2 is for the input filter for the PCC voltage measurement which is slightly larger than for the reactive current controller.

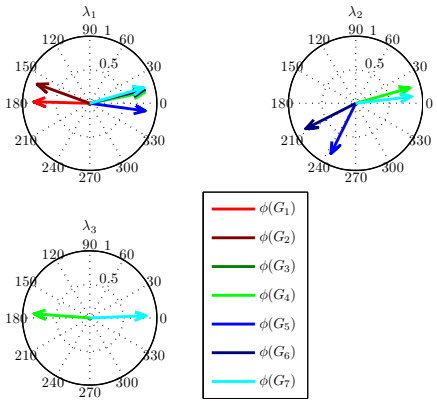

Fig. 13. Mode shape for the generator speed state for three inter-area modes. The presented mode shapes are for case 1 with $P_{\text{WPP}} = 1\,000$ MW and with a WPP voltage controller in service.

TABLE VII
COMPARISON OF SELECTED PARTICIPATION FACTORS FOR INTER-AREA MODE, λ_1, FOR CASE 1 AND 2. FOR THE WPP PARTICIPATION FACTORS ARE SHOWN FOR MECHANICAL GENERATOR-, ROTOR- AND SHAFT-ANGLE STATES, AND THE MAXIMUM PARTICIPATION OVER ALL WPP STATES. $P_{\text{WPP}} = 1\,000$ MW.

State variables	$\lvert p_{j1}\rvert$ case 1	$\lvert p_{j1}\rvert$ case 2
δ (G_1)	0.22	0.28
δ (G_2)	0.10	0.04
δ (G_3)	$< 10^{-2}$	$< 10^{-2}$
δ (G_4)	0.03	0.03
δ (G_5)	0.03	0.03
δ (G_6)	0.08	0.07
δ (G_7)	0.01	0.01
δ_g (WPP)	$< 10^{-7}$	$< 10^{-7}$
δ_r (WPP)	$< 10^{-5}$	$< 10^{-5}$
δ_s (WPP)	$< 10^{-5}$	$< 10^{-5}$
$\max_{\mathbf{x}}(\lvert p_1\rvert)$ (WPP)	$< 10^{-2}$	$< 10^{-2}$

V. DISCUSSION

This paper presents a modal analysis of full-load converter interfaced WTs. Focus of the work is the impact increased wind power penetration has on power system inter-area oscillations. The study is based on a 18 node, 7 generator power system model to which the WPP is connected. The system model represents a large network with a reduced number of nodes and has been developed in collaboration with National Grid to assist in the understanding of power oscillations between major areas of the UK power system. The attached WPP is modeled as an aggregated machine which includes all grid significant components [29]. The WPP is furthermore equipped with a voltage controller that controls the voltage at the interface to the external grid.

To accommodate the production from additional generation units, assuming that load and power transfer to neighboring systems does not increase, the production from the existing units should decrease accordingly to keep the power balance. Two ways this can happen are *1)* all units stay connected but with reduced active power output, or *2)* a proportion of the existing units are taken out of service to ensure good utilization of the units in service.

Three inter-area modes are monitored as the penetration of wind power increases, and both with and without WPP voltage controller the inter-area modes seem largely unaffected by the increased capacity of the WPP. Comparing the inter-area characteristics in TABLE II, IV, and VI it is noted that the damping of the three inter-area modes is almost constant, while the frequency of oscillation, especially for λ_1, increases slightly. For inter-area mode λ_1 the damped frequency of oscillation increases by 4 % in case 2 where the synchronous generator, G_2, is being displaced by the WPP.

The WPP voltage controller does not significantly change the modal properties of the system. A comparison of the results in section IV-A and IV-B shows a large degree of uniformity, with the trajectories in the complex plane in Fig. 10 and 12 being almost identical.

The degree of interaction of the WPP in the power system oscillations is evaluated with the aid of participation factors. The participation in the system oscillations of the WPP mechanical system are orders of magnitude smaller than those computed for the synchronous machines. This could imply a decoupling between the grid dynamics and the WPP mechanical system by the full-load converter.

VI. Conclusion

In this paper a modal analysis is presented where the impact of full-load converter interfaced wind turbines on power system oscillations is evaluated. The analysis is repeated for various wind power penetration levels, two different strategies for accommodating the wind energy, and with and without a wind power plant voltage controller.

The study found that the inter-area modes were largely unaffected by the increased capacity of the wind power plant. The damping of three selected inter-area modes was almost unchanged for the analyzed cases while smaller increases, < 4 %, were seen in the damped frequency of oscillation.

Generally, a very small participation from the wind turbines was found in the system oscillatory modes, hence implying that the wind power plant does not interact with these system modes.

Appendix A
System Parameters

TABLE VIII
Generator ratings, transformer reactances, and load characteristics. Transformer rating is same as generator rating and the reactance is given on this base.

Generators [MVA]		Transformers [%]		Loads [MVA]	
G_1	3 000	T_1	$X_L = 16$	L_3	$755 + j220$
G_2	2 400	T_2	$X_L = 16$	L_4	$4\,320 + j1\,580$
G_3	1 000	T_3	$X_L = 16$	L_5	$3\,200 + j954$
G_4	7 300	T_4	$X_L = 16$	L_6	$6\,310 + j2\,030$
G_5	2 900	T_5	$X_L = 16$	L_7	$2\,910 + j960$
G_6	5 500	T_6	$X_L = 16$	L_8	$2\,500 + j775$
G_7	2 800	T_7	$X_L = 16$		

TABLE IX
Machine parameters for all synchronous generators on machine base.

	G_1	G_2	G_3	G_4	G_5	G_6	G_7
H [s]	4.237	4.464	4.358	5.562	5.474	4.879	4.066
D [s]	0	0	0	0	0	0	0
R_s [pu]	0.002	0.001	0.010	0.001	0.002	0.001	0.002
X_l [pu]	0.167	0.187	0.167	0.169	0.167	0.180	0.183
X_d [pu]	2.360	2.116	2.001	2.470	2.235	2.158	2.510
X_q [pu]	2.261	2.043	1.937	2.301	2.113	2.069	2.447
X'_d [pu]	0.297	0.312	0.293	0.278	0.269	0.300	0.313
X'_q [pu]	0.297	0.312	0.293	0.278	0.609	0.300	0.313
X''_d [pu]	0.209	0.250	0.219	0.203	0.198	0.227	0.226
X''_q [pu]	0.209	0.248	0.227	0.248	0.209	0.237	0.226
T'_{do} [s]	0.692	1.008	0.933	0.721	1.002	1.004	0.691
T'_{qo} [s]	0.692	1.008	0.933	0.721	1.002	1.004	0.691
T''_{do} [s]	0.031	0.023	0.036	0.019	0.032	0.065	0.026
T''_{qo} [s]	0.031	0.064	0.040	0.020	0.047	0.071	0.026

TABLE X
WPP collector network parameters for $P_{\text{WPP}} = 180$ MW

Network			Park trafo.
R [Ω]	X_L [Ω]	B_C [μS]	X_T [%]
0.086	0.070	3219.7	12.2

TABLE XI
Network parameters

	R [Ω]	X_L [Ω]	B_C [μS]
l_{18}	0	4.00	0
l_{28}	0	32.00	0
l_{38}	11.93	114.64	0
l_{48}	6.47	64.37	1189.91
l_{34}	0.40	4.91	1007.73
l_{47}	0.09	1.28	902.17
l_{57}	2.35	30.20	1512.05
l_{67}	0.38	4.88	1502.76
l_{56}	1.70	26.17	1475.95

References

[1] K. Belyeu. 2008: Another record year for wind energy installations. American Wind Energy Association. 1501 M Street, NW, Suite 1000, Washington, DC 20005, USA. [Online]. Available: http://www.awea.org/pubs/factsheets.html

[2] J. M. Mauricio, A. Marano, A. Gomez-Exposito, and J. L. Martinez Ramos, "Frequency regulation contribution through variable-speed wind energy conversion systems," *Power Systems, IEEE Transactions on*, vol. 24, no. 1, pp. 173–180, Feb. 2009.

[3] R. de Almeida and J. Lopes, "Participation of doubly fed induction wind generators in system frequency regulation," *Power Systems, IEEE Transactions on*, vol. 22, no. 3, pp. 944–950, Aug. 2007.

[4] J. Morren, J. Pierik, and S. W. de Haan, "Inertial response of variable speed wind turbines," *Electric Power Systems Research*, vol. 76, no. 11, pp. 980–987, 2006.

[5] P.-K. Keung, P. Li, H. Banakar, and B. T. Ooi, "Kinetic energy of wind-turbine generators for system frequency support," *Power Systems, IEEE Transactions on*, vol. 24, no. 1, pp. 279–287, Feb. 2009.

[6] V. Akhmatov, "Variable-speed wind turbines with doubly-fed induction generators part III: Model with the back-to-back converters," *Wind Engineering*, vol. 27, no. 2, pp. 79–91, 2003.

[7] ——, "Full-load converter connected asynchronous generators for MW class wind turbines," *Wind Engineering*, vol. 29, no. 4, pp. 341–351, 2005.

[8] ——, "Variable-speed wind turbines with doubly-fed induction generators. part IV: uninterrupted operation features at grid faults with converter control coordination," *Wind Engineering*, vol. 27, no. 6, pp. 519–29, 2003.

[9] J. Morren and S. de Haan, "Ridethrough of wind turbines with doubly-

fed induction generator during a voltage dip," *Energy Conversion, IEEE Transactions on*, vol. 20, no. 2, pp. 435–441, 2005.

[10] G. Rogers, *Power System Oscillations*, 1st ed., ser. Power Electronics and Power Systems. Kluwer Academic Publishers, 2000, iSBN-10: 0792377125.

[11] O. Anaya-Lara, F. Hughes, N. Jenkins, and G. Strbac, "Influence of windfarms on power system dynamic and transient stability," *Wind Engineering*, vol. 30, no. 2, pp. 107–27, 2006.

[12] E. Hagstrom, I. Norheim, and K. Uhlen, "Large-scale wind power integration in norway and impact on damping in the nordic grid," *WIND ENERGY*, vol. 8, no. 3, pp. 375–384, JUL-SEP 2005.

[13] J. Slootweg and W. Kling, "The impact of large scale wind power generation on power system oscillations," *Electric Power Systems Research*, vol. 67, no. 1, pp. 9 – 20, 2003.

[14] G. Tsourakis, B. Nomikos, and C. Vournas, "Effect of wind parks with doubly fed asynchronous generators on small-signal stability," *Electric Power Systems Research*, vol. 79, no. 1, pp. 190 – 200, 2009. [Online]. Available: http://www.sciencedirect.com/science/article/B6V30-4T0FHRM-1/2/3b6ac71f22cac8ff81670dcc6944a0f9

[15] A. Tabesh and R. Iravani, "Small-signal dynamic model and analysis of a fixed-speed wind farm-a frequency response approach," *Power Delivery, IEEE Transactions on*, vol. 21, no. 2, pp. 778–787, 2006, iSSN: 0885-8977.

[16] ——, "Small-signal model and dynamic analysis of variable speed induction machine wind farms," *Renewable Power Generation, IET*, vol. 2, no. 4, pp. 215–227, December 2008.

[17] F. Hughes, O. Anaya-Lara, N. Jenkins, and G. Strbac, "A power system stabilizer for dfig-based wind generation," *Power System, IEEE Transactions on*, vol. 21, no. 2, pp. 763–772, 2006.

[18] Z. Miao, L. Fan, D. Osborn, and S. Yuvarajan, "Control of dfig based wind generation to improve inter-area oscillation damping," *Power and Energy Society General Meeting - Conversion and Delivery of Electrical Energy in the 21st Century, 2008 IEEE*, pp. 1–7, July 2008.

[19] P. Ledesma and C. Gallardo, "Contribution of variable-speed wind farms to damping of power system oscillations," *2007 IEEE Lausanne Power Tech*, pp. 190–194, 2007.

[20] A. Mendonca and J. Lopes, "Robust tuning of power system stabilisers to install in wind energy conversion systems," *Renewable Power Generation, IET*, vol. 3, no. 4, pp. 465–475, December 2009.

[21] K. Elkington, "Modelling and control of doubly fed induction generators in power systems: Towards understanding the impact of large wind parks on power system stability," Ph.D. dissertation, KTH, Electric Power Systems, 2009, iSBN: 978-91-7415-264-7. [Online]. Available: http://urn.kb.se/resolve?urn=urn:nbn:se:kth:diva-10206

[22] M. Klein, G. Rogers, and P. Kundur, "A fundamental study of inter-area oscillations in power systems," *Power System, IEEE Transactions on*, vol. 6, no. 3, pp. 914–921, 1991.

[23] P. S. Kundur, *Power System Stability and Control*, ser. The EPRI Power System Engineering Series. McGraw-Hill, Inc., 1994, ISBN: 0-07-035958-X.

[24] D. Trudnowski, "Estimating electromechanical mode shape from synchrophasor measurements," *Power Systems, IEEE Transactions on*, vol. 23, no. 3, pp. 1188–1195, Aug. 2008.

[25] D. Trudnowski, J. Hauer, J. Pierre, W. Litzenberger, and D. Maratukulam, "Using the coherency function to detect large-scale dynamic system modal observability," in *American Control Conference, 1999. Proceedings of the 1999*, vol. 4, 1999, pp. 2886–2890 vol.4.

[26] A. R. Messina, Ed., *Inter-area Oscillations in Power Systems: A Nonlinear and Nonstationary Perspective*. Springer Publishing Company, Incorporated, 2009, iSBN: 978-0-387-89529-1.

[27] J. Sanchez-Gasca, V. Vittal, M. Gibbard, A. Messina, D. Vowles, S. Liu, and U. Annakkage, "Inclusion of higher order terms for small-signal (modal) analysis: committee report-task force on assessing the need to include higher order terms for small-signal (modal) analysis," *Power Systems, IEEE Transactions on*, vol. 20, no. 4, pp. 1886–1904, Nov. 2005.

[28] ——, "Analysis of higher order terms for small signal stability analysis," in *Power Engineering Society General Meeting, 2005. IEEE*, June 2005, pp. 1745–1753 Vol. 2.

[29] J. N. Nielsen, V. Akhmatov, J. Thisted, E. Grøndahl, P. Egedal, M. N. Frydensbjerg, and K. H. Jensen, "Modelling and fault-ride-trough tests of siemens wind power 3.6 mw variable-speed wind turbines," *Wind Engineering*, vol. 31, pp. 441–452(12), December 2007. [Online]. Available: http://www.ingentaconnect.com/content/mscp/wind/2007/00000031/00000006/art00006

[30] N. G. plc, "The grid code," National Grid Electricity Transmission plc, National Grid House, Warwick Technology Park, Gallows Hill, Warwick, CV34 6DA, UK, Tech. Rep. Issue 4 Revision 2, March 2010.

Thyge Knüppel received his M.Sc.E.E. degree from the Technical University of Denmark (DTU) in the spring of 2008 where he specialized in power systems and control theory. Currently, he is employed as research engineer at Siemens Wind Power A/S and is pursuing a PhD degree from DTU.

Vladislav Akhmatov holds M.Sc. (1999) and Ph.D. (2003) degrees from the Technical University of Denmark, Kgs. Lyngby, Denmark. He has been with the Danish power company NESA, now part of DONG Energy, the Danish transmission system operator Energinet.dk, Centre for Electric Technology at the Technical University of Denmark, and at present he is a Senior Engineer and Chief Specialist with the wind turbine manufacturer Siemens Wind Power. His main interests are wind turbine modeling, wind power grid-integration, power system modeling, operation and stability. He has authored and co-authored several papers and books on the topics of interests.

Jørgen N. Nielsen holds M.Sc. (1996) and Ph.D. (2000) degrees from the Technical University of Denmark, Kgs. Lyngby, Denmark. He has a broad and comprehensive knowledge and experience on power system planning, network investigations and power system simulations. Jørgen N. Nielsen has performed and been responsible for a number of network investigations and studies issued the integration of wind power in the power system and been deeply involved into the development of numerical PSS/E simulation models of the fixed- and variable-speed wind turbines.

Kim H. Jensen holds M.Sc. (1999) and Ph.D. (2003) degrees from the Technical University of Denmark, Kgs. Lyngby, Denmark. He has been working in a transmission company (NESA), consultant company (Elsam Engineering) and now a wind turbine company (Siemens Wind power). In these companies he has worked with transmission system planning, network designs, wind turbine modelling, grid codes studies and harmonic analysis and stability studies. He has also worked as technical specialist on an number wind farm integration projects.

Andrew Dixon holds B.Sc. and Ph.D. degrees in Applied Mathematics (1984. 1988) from the University of St Andrews, Scotland and an M.Sc. in Electric Power Systems (2005) from the University of Bath, England. Dr. Dixon has worked for 19 years for the National Grid Company, UK, consisting of: Research & Development (security-constrained optimization of reactive compensation) - 2 years; System Development & Grid Code - 6 years; Operational Planning - 4 years; Asset Management - 2 years; System Technical Performance (dynamics, including transient stability, small-signal stability & sub-synchronous resonance) - 5 years.

Jacob Østergaard is professor in Electric Technology, Head of Centre for Electric Technology (CET) and Head of Section for Electric Power Engineering at the Department of Electrical Engineering, DTU. From 1995 to 2005 he worked as research engineer and area responsible at Research Institute for Danish Electric Utilities (DEFU). Current activities include research within electricity production, transmission, distribution and demand. Prof. Østergaard is presently involved in activities related to an intelligent power system with focus of new electricity and information architectures, system integration of distributed generation and increased flexibility in the power system by use of demand side participation. Prof. Østergaard is project leader of more than 10 research projects. and serves in several professional organizations including the EU SmartGrids advisory council.